IDENTIFICATION OF HYDROGEOCHEMICAL PROCESSES IN GROUNDWATER USING MAJOR ION CHEMISTRY: A CASE STUDY OF YENAGOA AND ENVIRONS, SOUTHERN NIGERIA

KENNETH S. OKIONGBO AND EDIRIN AKPOFURE

ABSTRACT

Hydrogeochemical studies were carried out in Yenagoa city and environs, Southern Nigeria in order to assess the chemistry of the groundwater and identify the dominant hydrogeochemical processes and mechanisms responsible for the evolution of the chemical composition of the groundwater. The study approach includes detailed geochemical analysis of groundwater samples collected from domestic boreholes for major constituents such as Ca^{2+}, Mg^{2+}, Na^+, K^+, HCO_3, Cl^-, SO_4^{2-}, and NO_3^- and the hydrochemical data was subjected to multivariate statistical analysis and conventional graphical plots. The results show that most groundwater quality parameters are within World Health Organization acceptable limits for drinking water. The chemical relationships of the ions in Piper diagram identify Ca-Cl, Ca-HCO_3 and Na-HCO_3 as most prevalent water types. The alkalis exceed the alkaline earths and weak acids exceed the strong acids. The contribution of (Ca + Mg) and (Na + K) to total cations and HCO_3 indicates the dominance of silicate weathering as the major source of cations. The plot of Na vs Cl indicates higher Na, derived from silicate weathering process which was also supported by higher HCO_3 values. Reverse ion exchange process is also significant in the study area which is indicated by negative Schoeller indices and shifting to the left in the plot of $Ca^{2+} + Mg^{2+}$ vs $HCO_3 + SO_4$. Furthermore, the plot of Na-Cl vs Ca+Mg – HCO_3 – SO_4 confirms that Ca, Mg, and Na concentrations in groundwater are derived from aquifer materials. Saturation index of silicate and carbonate minerals indicate undersaturation to oversaturation

KEYWORDS: Groundwater, ion exchange, rock-water interaction, saturation index, Yenagoa

INTRODUCTION

Groundwater flows through geological materials as it moves along its path from recharge to discharge areas. As a result of the hydrogeochemical processes such as dissolution, precipitation, ion-exchange processes that occur in such flow and as well as the residence time along the flow path, groundwater contains a wide variety of dissolved inorganic chemical constituents. The type and concentration of these constituents depend upon several factors including the composition of the precipitation, geological structure and mineralogy of the watersheds and aquifers and the geological processes within the aquifer (Andre et al., 2005). Thus, hydrogeochemical composition of groundwater can be indicative of the origin and history of its spatial flow.

It has been shown that the geochemical processes are responsible for the seasonal and spatial variations in groundwater chemistry (Kumar et al., 2009). Evaluation of the groundwater chemistry and delineation of various hydrogeochemical processes that are involved in the evolution of groundwater quality using various conventional graphical methods and interpreting different indices were carried out by many workers in the recent past (Elango et al., 2003). These workers reported that hydrogeochemical processes control the chemical composition of groundwater and concluded that the character of groundwater in different aquifers over space and time is an effective tool in solving different geochemical problems. Thus, knowledge of hydrogeochemical processes that control groundwater chemical evolution could lead to improved understanding of hydrogeochemical characteristics of an aquifer. This could contribute to sustainable development of water resources and effective management of groundwater as a resource.

Some of the previous studies carried out in Yenagoa and environs, include groundwater quality assessment (Amadi et al., 1987; Okiongbo and Douglas, 2013). These studies, however, did not attempt to identify the hydrogeochemical processes that control the groundwater chemistry of the area. As a fast growing urban centre, groundwater is the major and preferred source of water for domestic and irrigation purposes. It is thus essential to understand the hydrogeochemical processes that are taking place in the aquifer system. Hence the present study was carried out with the objective of assessing the water chemistry and to identify the hydrogeochemical processes that control the chemistry of the groundwater in the study area.

Description of the Study Area
The study area lies between longitudes 006° 05´ and 00 6° 040´ East of the prime meridian and latitudes 04° 23.3´ and 04° 38.2´ North of the equator within the

Kenneth S. Okiongbo, Department of Geology & Physics, Niger Delta University, Wilberforce Island, Bayelsa State, Nigeria

Edirin Akpofure, Department of Geology & Physics, Niger Delta University, Wilberforce Island, Bayelsa State, Nigeria

coastal area of the recent Niger Delta (Fig. 1). It has an areal extent of about 100 km^2 and has a tropical rain forest climate with two distinct seasons; wet (April-October) and dry (November-March). The mean annual rainfall is around 4500mm with about 85% in the wet season serving as the major source of groundwater recharge (Akpokodje, 1986). There are a number of perennial streams, oxbow lakes and rivers in the area, (e.g Kolo Creek, Epie Creek, Yenagoa and Nun river, etc.). They all form a network which empties to the Atlantic Ocean through Nun River Estuary. This area is usually submerged during the wet season where flood waters range from 0.5 to 4m deep (Akpokodje, 1986).

The vegetation comprises of evergreen trees and oil palms. In addition, there are smaller climbing plants, parasitic plants that live on other plants. More than 70% of the inhabitants of the study area are engaged in subsistent farming and fishing.

Geology and Hydrogeology
The study area (Fig.1) lies within the fresh water, swamp forest and backswamps geomorphic unit of the Niger Delta. The Niger Delta is basically an alluvial plain formed by the deposition and built – up of fine grained sediments eroded and transported to the area by the River Niger and its tributaries.
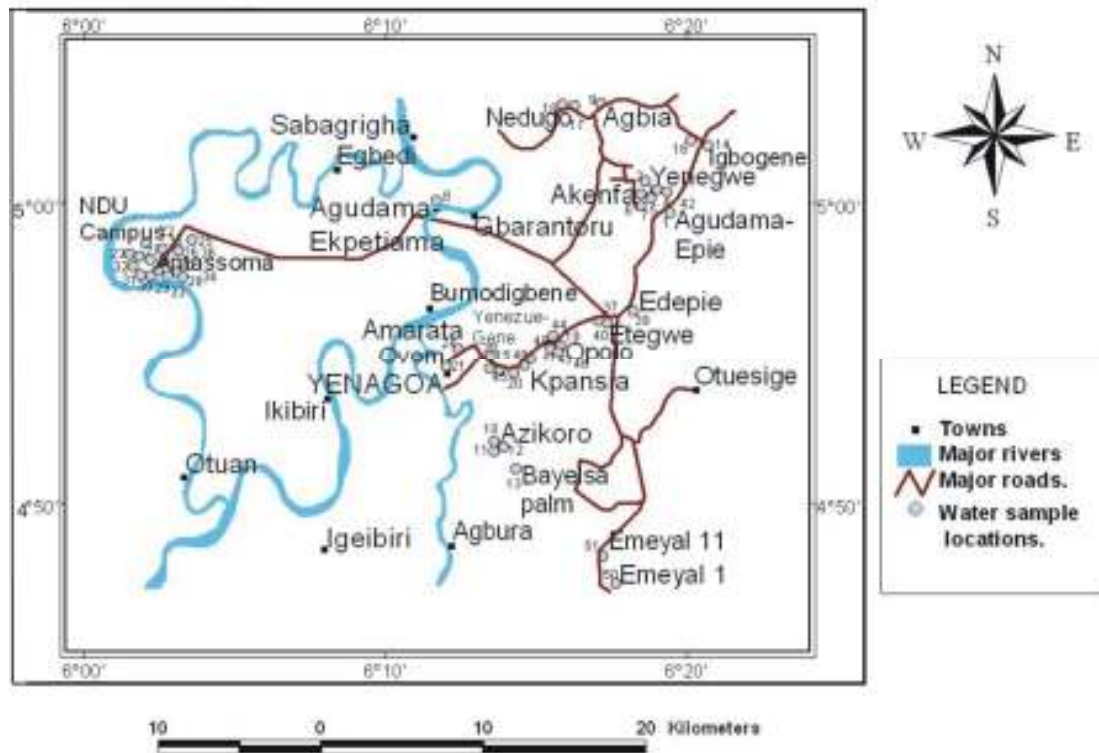

Fig.1: Map of study area showing the borehole locations

The regional geology of the Niger Delta is relatively simple; consisting of three lithostratigraphic units, Akata, Agbada and Benin Formations, overlain by various types of Quaternary deposits (Short and Stauble, 1967).

The quaternary deposits are considered universally to be recent expressions of and continuation of the Benin Formation and consist of medium to coarse-grained sands, sandy clays, silts and subordinate, lensoid clay bands thought to have been deposited during quaternary interglacial marine transgressions (Durotoye, 1989). Amajor (1991) has shown that they are an admixture of fluvial/tidal channel, tidal flats and mangrove swamp deposits. The sands are micaceous and feldspathic, subrounded to angular in texture and constitute good aquifers. However, depth to occurrence and thickness is irregular and may not be

predicted with accuracy within the study area due to rapid horizontal and vertical facie changes. Groundwater occurs generally under water table conditions where the lensoid clays attain adequate thickness.

The Benin Formation is essentially fluvial in origin comprising unconsolidated, massive and porous fresh water bearing sands with localized clay/shale beds. The sand – clay intercalations are indicative of a multi – aquifer system. The thickness of the Benin Formation is about 2100 m on the average. The age of this Formation ranges from Miocene to Recent. Water table in large sections of the Niger Delta is close to the surface but subject to spatial and seasonal variations. In the study area, the water table is about 3 – 4 m during the dry season. During the wet season, the water table rises considerably, in some cases, to the ground surface. The Agbada Formation underlies the Benin

Formation. Its thickness varies from 300 – 4500 m (Short and Stauble, 1967). This Formation consists predominantly of unconsolidated pebbles, and very coarse to fine grained sand units with subordinate shale beds. Underneath the Agbada Formation is the Akata Formation of Eocene to recent age (Amadi et al. 1987), which is made up of shales with local inter-bedding of sands and siltstones. It was deposited in a marine environment with maximum thickness of about 6100m (Ofoegbu, 1985).

METHOD OF STUDY

Groundwater samples were collected from 51 representative domestic boreholes (Fig.1) spread over the study area during the month of March, 2013. The samples were collected in polyethylene bottles for the laboratory analysis of major ions such as Na, K, Ca, Mg and HCO_3, CO_3, Cl, and SO_4 using standard procedures (APHA 1995).   Electrical Conductivity and pH of groundwater samples were measured in the field immediately after sample collection using portable field kits (Hach's CO 150 Conductivity/TDS meter and pH meter respectively). Major ions like chlorides, bicarbonates, calcium, and magnesium were analysed by titration. Sodium and potassium were measured by a flame photometer, while the sulfates were estimated by the visible- UV spectrophotometer. In general, the ion balance error of the samples was observed to be within the range of ±10%.

The data were analysed using the multivariate statistical technique (Principal Component Analysis). Aside, the potential for a chemical reaction to occur within an aquifer was determined by calculating the chemical equilibrium of the water with the mineral phases in question. The equilibrium state of the water with respect to a mineral phase can be determined by calculating a saturation index (SI) using analytical data. The potential for mineral precipitation or dissolution could be assessed using the saturation index (SI), which is based on the relation between analytic activities (the ion activity product, IAP) and the thermodynamic calculation of the solubility product (*K*s). The SI of a mineral can be determined using the following equation:

$$SI = \log\left(\frac{IAP}{K_S}\right)$$

If SI > 0, the solution is theoretically oversaturated with respect to the mineral and precipitation is expected. For SI = 0, the mineral and solution are in equilibrium and neither dissolution nor precipitation is expected to occur. If SI < 0, the solution is theoretically undersaturated with respect to the mineral, and if present in the system, dissolution might be possible. The saturation indices of the groundwater with respect to the mineral phases were determined using the geochemical modelling programme PHREEQC (Parkhurst and Appelo, 1999).

RESULTS AND DISCUSSION

Hydrogeochemical characteristics and groundwater Quality

The results of the chemical constituents of the groundwater samples are shown in Table 1. Table 2 gives the statistical variation of the various investigated parameters. These were compared with World Health Organisation standards (WHO, 2004). The results show that pH ranges from 5.55 to 6.93 with a mean of 6.13, indicating that the groundwater is mildly acidic in the study area. Electrical conductivity values indicate the amount of total dissolved salts, which in turn indicates the inorganic pollution load of the water. The electrical conductivity values range from 102 to 2820µS/cm. Table 1 shows that over 90% of the total groundwater samples were within the maximum permissible limits of 1400 µS/cm. The TDS, which is a measure of the degree of groundwater quality, is in the range of 51 to 1410mg/L with a mean of 388.3mg/L. Davis and De Wiest (1966), classified groundwater on the basis of TDS, up to 500mg/L (desirable for drinking); 500 – 1,000mg/L (permissible for drinking) and up to 3,000mg/L (useful for agricultural purposes). Based on this classification, it is observed that out of 51 samples analysed, 36 are desirable for drinking, 11 are allowable for drinking and 4 are useful for agricultural purposes. Total hardness (TH) in the study area ranges from 3 to 265mg/L. Based on TH, Dufor and Becker (1964), classified water as 0 – 60, soft; 61 – 120, moderately hard; 121 – 180, hard; and > 180 very hard water. About 78% of our samples belong to the soft type, 12% belong to the moderately hard type, 4% to the hard type and 6% to very hard type. Table 1 shows that about 71% of groundwater samples have TH more than TA, which implies that the groundwater is characterised by noncarbonated hardness (Chow, 1964). The concentrations of sodium in the samples ranged from 1.1 to 60.4mg/L with a mean of 17.4mg/L. Potassium concentration ranged from 1.02 to 30.4mg/L with a mean of 9.9mg/L. Calcium concentration ranged from 1.2 to 40.5mg/L with a mean of 9.9mg/L. Magnesium concentration ranged from 0.5 to 21.8mg/L with a mean of 5.2mg/L. The concentration of iron ranged from 0.01 to 12.3mg/L with a mean of 3.2mg/L.   Chloride concentrations in the samples were from 2.9 to 54.8 mg/L with a mean value of 19.2 mg/L.

Table 1: Hydrogeochemical Analysis of Groundwater Samples

S/N	Code	pH	EC	TDS	TA	TH	Na^+	K^+	Ca^{2+}	Mg^{2+}	Fe	Cl^-	SO_4^{2-}	NO_3^-	HCO_3	CAI-1	CA1-2	SO4/Cl
1	BH1	6.83	2120.0	1060.0	55.0	143.0	52.2	30.4	40.5	10.7	0.50	31.8	7.2	0.13	300.8	-2.4	-0.4	0.2
2	BH2	6.16	338.0	169.0	15.0	48.0	14.2	6.8	2.4	0.5	0.02	2.9	0.5	0.11	52.5	-8.9	-0.8	0.2
3	BH3	5.78	615.0	308.0	26.0	25.0	28.4	16.5	4.0	0.8	0.01	4.8	4.2	0.08	103.7	-11.2	-0.9	0.9
4	BH4	5.87	472.0	236.0	16.0	16.0	14.5	12.0	6.1	3.5	0.18	4.6	1.2	0.08	84.2	-6.2	-0.6	0.3
5	BH5	6.17	400.0	200.0	20.0	6.0	18.2	9.9	5.4	3.1	0.15	12.5	1.8	0.04	72.0	-2.0	-0.6	0.1
6	BH6	5.82	768.0	384.0	39.0	50.0	16.5	6.8	5.5	2.5	0.24	5.5	4.6	0.27	68.3	-4.7	-0.6	0.8
7	BH7	6.03	515.0	256.0	21.0	44.0	18.4	7.5	3.5	1.2	0.18	4.8	1.7	0.16	67.1	-6.3	-0.8	0.4
8	BH8	6.38	708.0	354.0	30.0	48.0	28.4	9.5	6.8	3.4	0.12	17.3	2.8	0.03	94.6	-2.0	-0.6	0.2
9	BH9	6.20	2620.0	1310.0	48.0	254.0	60.4	28.5	36.4	8.5	0.02	82.0	5.7	0.13	209.8	-0.5	-0.3	0.1
10	BH10	6.24	800.0	400.0	28.0	40.0	14.5	8.7	5.6	3.5	0.25	11.3	0.9	0.16	66.5	-1.7	-0.5	0.1
11	BH11	6.15	1036.0	518.0	24.0	40.0	29.5	18.4	6.3	2.7	0.05	14.4	3.2	0.14	111.0	-3.3	-0.7	0.2
12	BH12	5.92	907.0	454.0	42.0	57.0	25.5	15.6	8.5	2.2	0.29	14.8	4.2	0.05	98.2	-2.6	-0.6	0.3
13	BH13	6.16	696.0	348.0	42.0	52.0	12.5	8.2	4.5	5.6	0.32	14.5	2.5	0.01	60.4	-0.8	-0.3	0.2
14	BH14	5.80	1091.0	546.0	33.0	120.0	42.2	17.6	5.5	2.3	0.18	21.2	4.0	0.09	126.9	-2.8	-0.8	0.2
15	BH15	6.31	418.0	209.0	30.0	15.0	12.2	10.5	6.74	3.46	0.25	16.0	0.54	0.09	59.2	-0.8	-0.4	0.0
16	BH16	5.87	1324.0	662.0	60.0	54.0	41.7	18.4	12.8	8.8	0.21	20.4	3.5	0.14	183.0	-3.0	-0.6	0.2
17	BH17	5.87	1098.0	549.0	40.0	48.0	15.4	9.8	10.7	6.2	0.31	21.6	10.6	0.00	70.2	-0.5	-0.2	0.5
18	BH18	6.00	440.0	220.0	39.0	23.5	15.2	7.4	4.6	2.5	0.38	11.7	5.5	0.28	51.9	-1.6	-0.5	0.5
19	BH19	6.04	207.0	104.0	13.0	14.2	3.8	2.5	2.9	1.6	0.32	10.3	2.1	0.20	11.0	0.2	0.3	0.2
20	BH20	6.34	2820.0	1410.0	65.0	265.0	48.7	15.2	20.9	6.9	0.18	39.1	6.5	0.42	175.7	-1.3	-0.5	0.2
21	BH21	6.88	792.0	396.0	30.0	68.0	18.8	8.2	8.0	1.8	0.18	8.4	5.4	0.15	70.0	-3.4	-0.6	0.6
22	BH22	6.18	495.0	248.0	18.0	42.0	13.8	6.5	3.5	1.8	0.86	14.2	4.7	1.60	36.0	-0.9	-0.5	0.3
23	BH23	6.19	409.0	205.0	32.0	23.0	17.2	8.3	5.0	4.5	0.28	6.9	2.6	0.05	81.7	-3.9	-0.5	0.4
24	BH24	6.70	591.0	296.0	26.0	24.0	7.8	12.0	5.7	4.2	0.20	5.3	3.3	0.28	64.7	-3.3	-0.4	0.6
25	BH25	6.06	910.00	455.00	23.00	60.00	12.40	7.60	13.50	3.80	10.10	12.50	2.30	6.74	8.40	-1.08	-1.15	0.2
26	BH26	5.80	890.00	450.00	17.00	85.00	10.60	5.80	14.80	12.60	2.08	28.40	1.20	1.68	6.20	0.24	1.17	0.0
27	BH27	6.20	1060.00	530.00	22.00	57.00	12.50	10.50	28.50	21.80	11.94	49.70	3.00	5.85	10.80	0.42	1.60	0.1
28	BH28	6.22	1200.00	600.00	26.00	75.00	9.50	12.60	18.80	6.70	12.00	17.70	5.40	8.56	18.20	-0.47	-0.40	0.3

S/N	Code	pH	EC	TDS	TA	TH	Na^+	K^+	Ca^{2+}	Mg^{2+}	Fe	Cl^-	SO_4^{2-}	NO_3^-	HCO_3	CAI-1	CA1-2	SO4/Cl
29	BH29	6.19	690.00	345.00	16.00	55.00	8.50	4.60	15.70	6.50	10.61	24.50	1.10	1.50	5.60	0.29	1.38	0.0
30	BH30	6.44	1163.00	582.00	26.00	65.00	12.30	6.40	16.50	10.80	6.06	21.30	6.50	2.45	14.80	-0.16	-0.23	0.3
31	BH31	6.46	1089.00	545.00	15.00	75.00	8.80	9.20	15.20	8.00	7.38	14.20	4.80	3.40	9.40	-0.54	-0.66	0.3
32	BH32	6.65	1138.00	569.00	18.00	166.00	10.50	9.60	8.80	6.50	6.24	12.40	3.50	1.30	8.80	-1.01	-1.44	0.3
33	BH33	6.04	526.00	520.00	25.00	4.00	8.40	9.60	6.80	7.20	12.00	10.50	0.50	2.70	12.70	-1.06	-1.14	0.0
34	BH34	6.38	1068.00	534.00	15.00	73.00	7.40	7.50	10.20	5.80	12.08	17.00	0.84	4.85	10.50	-0.07	-0.12	0.0
35	BH35	6.84	591.00	296.00	38.00	37.00	6.50	7.80	10.80	8.20	9.08	30.40	0.38	2.20	4.00	0.44	3.08	0.0
36	BH36	6.93	593.00	297.00	10.00	15.00	6.40	7.40	2.80	6.90	12.10	15.00	0.54	3.70	3.80	-0.11	-0.29	0.0
37	BH37	6.31	2250.00	1125.00	42.00	260.00	38.90	14.00	15.00	5.70	12.26	18.50	12.40	4.60	40.00	-2.93	-1.51	0.7
38	BH38	6.02	277.00	139.00	12.40	13.50	15.60	10.50	10.20	6.40	1.20	21.00	8.40	0.32	4.80	-0.60	-1.36	0.4
39	BH39	5.72	191.00	96.00	8.60	6.80	8.50	4.60	5.40	3.20	3.40	9.80	3.80	0.12	2.80	-0.76	-1.65	0.4
40	BH40	5.77	508.00	254.00	14.50	15.00	17.70	14.20	12.60	6.80	0.15	19.90	15.40	0.35	8.60	-1.02	-1.22	0.8
41	BH41	6.00	331.00	165.00	15.00	19.00	8.50	6.70	11.40	7.60	0.22	22.80	14.60	0.16	6.20	0.16	0.25	0.6
42	BH42	5.78	201.00	100.00	13.50	16.70	7.50	5.40	8.60	4.80	4.60	18.20	13.60	0.15	5.80	0.09	0.13	0.7
43	BH43	5.70	323.00	162.00	14.20	9.80	26.50	12.70	6.25	3.24	5.20	22.20	16.50	0.13	6.90	-1.36	-1.85	0.7
44	BH44	5.69	348.00	174.00	15.10	14.00	18.30	10.88	8.94	6.41	2.50	20.00	15.40	0.29	7.20	-0.91	-1.15	0.8
45	BH45	5.71	335.00	168.00	12.00	11.70	7.80	4.10	7.52	4.70	3.40	17.70	15.30	0.20	6.70	0.11	0.13	0.9
46	BH46	5.64	119.00	60.00	2.50	3.50	3.80	3.50	3.40	2.85	4.80	16.50	9.54	0.12	3.80	0.45	0.80	0.6
47	BH47	5.86	161.00	82.00	3.80	4.70	1.07	4.70	4.85	3.42	2.60	18.50	9.35	0.14	2.80	0.68	1.45	0.5
48	BH48	6.16	102.00	51.00	2.00	7.50	1.42	1.02	1.20	0.85	0.38	19.10	0.85	0.15	1.60	0.84	9.54	0.0
49	BH49	5.55	294.00	147.00	13.00	12.60	4.28	1.85	3.50	2.80	0.25	12.30	12.60	0.28	5.50	0.33	0.32	1.0
50	BH50	6.35	112.00	60.00	2.20	3.00	2.80	2.00	2.40	1.60	0.42	36.50	16.72	0.07	2.00	0.83	2.23	0.5
51	BH51	6.33	909.00	455.00	28.50	18.60	38.50	12.60	18.50	6.70	3.50	54.80	28.80	0.28	14.50	-0.29	-0.54	0.5

All parameters have been expressed as mg/L, except pH and EC. The unit of EC is µS/cm while that of Total Alkalinity (TA) and Total Hardness (TH) is mg/L $CaCO_3$

Sulphate concentrations in these groundwater samples ranged from 0.5 to 28.8 mg/L with a mean value of 6.1mg/L. Nitrate concentrations ranged from 0.01 to 8.6 mg/L with a mean value of 1.12 mg/L. The bicarbonate anion concentrations were in the range of 6.2 to 300.8 mg/L with a mean value of 50.0 mg/L. The results obtained showed that the concentration of dissolved major cations and anions in the groundwater vary spatially and mass abundance was in the order of: Na^+ > Ca^{2+} > Mg^{2+} > K^+ > Fe for cations and HCO_3^- > Cl^- > SO_4^{2-} > NO_3^-.

Table 2: Descriptive Statistics of Analysed Groundwater Samples Compared with Standards

Parameter	No of Samples	Minimum	Maximum	Mean	Standard Deviation	WHO 2004 maximum permissible Limit
pH	51	5.55	6.93	6.13	0.34	6.5-8.5
EC (µS/cm)	51	102	2820	765.9	601.78	1400
TDS (mg/L)	51	51	1410	388.3	300.87	1000
TA (mg/L)	51	2	65	24.4	14.46	-
TH (mg/L)	51	3	265	53	62.60	500
Na^+ (mg/L)	51	1.1	60.4	17.4	13.65	200
K^+ (mg/L)	51	1.02	30.4	9.9	5.83	55
Ca^{2+} (mg/L)	51	1.2	40.5	9.9	8.05	75
Mg^{2+} mg/L)	51	0.5	21.8	5.2	3.66	50
Fe (mg/L)	51	0.01	12.3	3.18	4.27	0.3
Cl^- (mg/L)	51	2.9	54.8	19.2	13.80	250
SO_4^{2-} mg/L)	51	0.5	28.8	6.1	5.89	400
NO_3^- mg/L)	51	0.01	8.56	1.12	1.94	50
HCO_3^- mg/L)	51	6.2	300.8	50	62.13	-

The concentrations of these ions are below the World Health Organisation standard for drinking water in all samples except iron. The analytical data plotted on the EC versus SAR (sodium adsorption ratio = $Na^+/([Ca^{2+} + Mg^{2+}]/2)^{0.5}$ diagram (Fig. 2) illustrates that most of the groundwater samples fall in the field of C2-S1 and C3-S1 indicating medium to high salinity and low sodium water, which can be used for irrigation on almost all types of soil with little danger of exchangeable sodium (Karanth, 1989). The %Na^+ [percent Na^+ = (Na^+ + K^+) ×100/(Ca^{2+} + Mg^{2+} + Na^+ + K^+)] values indicate that about 65% of the groundwater is good to permissible for irrigation except a few samples falling in the field of doubtful and unsuitable for irrigation.
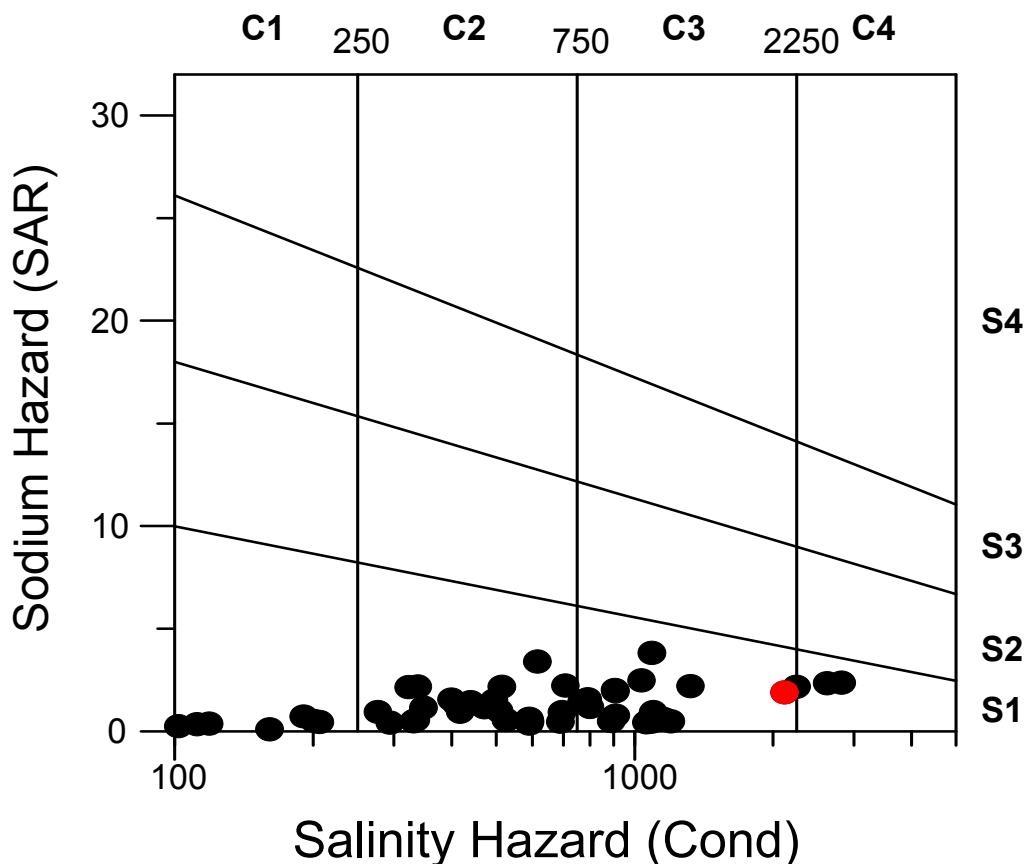
Fig.2: Wilcox salinity diagram

Principal component analysis was also used with the objective of establishing the associations between the physico-chemical variables and to note any correlation between them. Table 3 shows that the first three principal components together account for about 78.38% of the total variance in the data set, in which the first principal component explains 44.09% of the total variance, the second principal component exhibits 23.34% of the total variance and the third principal component exhibits 10.95% of the total variance.

Table 3: Rotated Principal Component Analysis Matrix of Chemical Data of Groundwater Samples

Chemical Variables	Principal Components			Communality
	I	II	III	
pH	0.351	0.297	0.401	0.372
EC	0.959	0.068	0.084	0.931
TDS	0.954	0.096	0.096	0.929
TA	0.791	-0.260	0.249	0.755
TH	0.842	0.060	0.121	0.727
Na^+	0.843	-0.416	-0.074	0.890
K^+	0.829	-0.280	0.002	0.765
Ca^{2+}	0.842	0.250	-0.302	0.863
Mg^{2+}	0.489	0.576	-0.325	0.676
Fe	0.070	0.903	0.003	0.820
Cl^-	0.616	0.112	-0.609	0.764
SO_4^{2-}	-0.019	-0.178	-0.851	0.756

NO^{3-}	0.177	0.867	0.117	0.796
HCO_3^-	0.743	-0.531	0.254	0.899
Eigenvalues	6.613	3.502	1.642	
% of variance explained by component	44.085	23.344	10.946	
Cumulative % of variance	44.085	67.429	78.375	

The first component reveals strong correlation between EC, TDS, TA, TH, Na^+, K^+, Ca^{2+}, Cl^-, and HCO_3. The second component shows a strong correlation between Fe and NO_3^-, while the third shows a strong correlation between Cl and SO_4. The combination of Na^+, K^+, Ca^{2+}, Mg^{2+}, Cl^-, and HCO_3 ions influencing the high positive loadings observed on the first principal component (Table 3) suggest that the first principal component is associated with a combination of hydrogeochemical processes that contribute to enrich more mineralized water.

The Piper trilinear diagram method (Fig. 3) was used to classify the groundwater, based on basic geochemical characters of the constituent ionic concentrations. On the basis of this diagram, groundwater in the study area was classified into three types mainly Ca-Cl, $Na-HCO_3$ and $Ca-HCO_3$. About 52.2% groundwater was dominated by the alkalis (Na^+ and K^+) over the alkaline earths (Ca^{2+} and Mg^{2+}) and in 54.2% of samples, weak acids (HCO_3^-) exceed strong acids (SO_4^- and Cl^-).
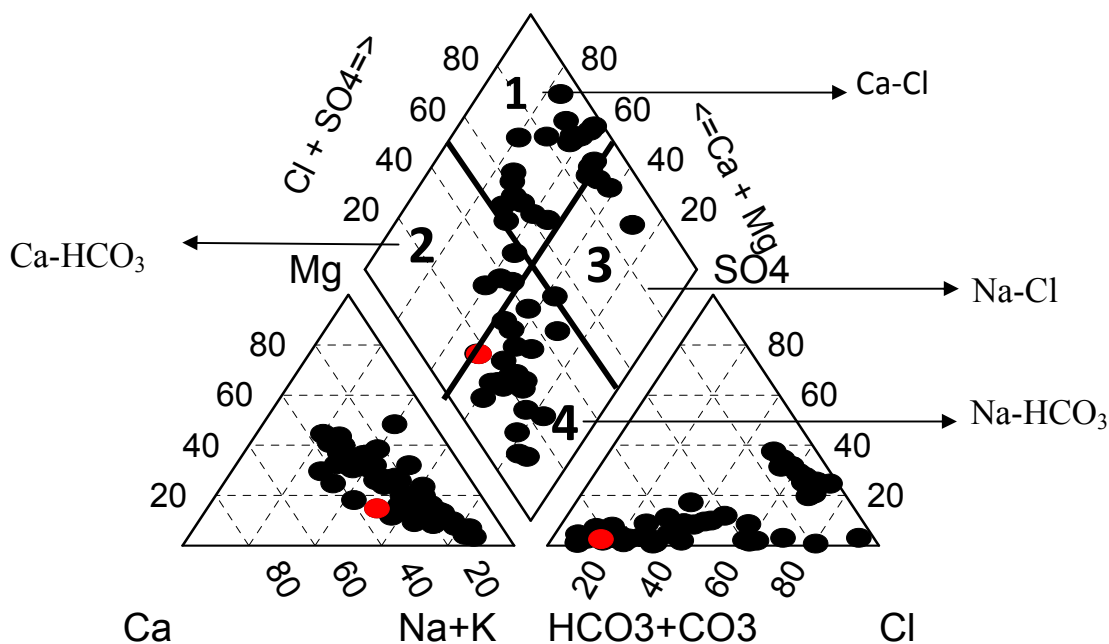
Fig.3: Piper trilinear diagram

Mechanism controlling groundwater chemistry
To assess the functional sources of dissolved chemical constituents, Gibb's diagrams were employed. These diagrams assess the functional sources of dissolved ions as precipitation dominance, rock dominance, and evaporation dominance, which control the water chemistry (Gibbs, 1970). Gibbs diagrams represent the ratios of $Na^+/(Na^+ + Ca^{2+})$ and $Cl^-/(Cl^- + HCO_3^-)$ as a function of TDS. The distribution of samples points in the

Gibb's diagram (Fig. 4) shows that the ratio of cations $Na^+/(Na^+ + Ca^{2+})$ and $Cl^-/(Cl^- + HCO_3^-)$ of the samples fall in the rock dominance zone suggesting precipitation induced chemical weathering along with dissolution of rock forming minerals. This suggests that chemical weathering of rock-forming minerals is the main causative factor in the evolution of chemical composition of groundwater in the study area.
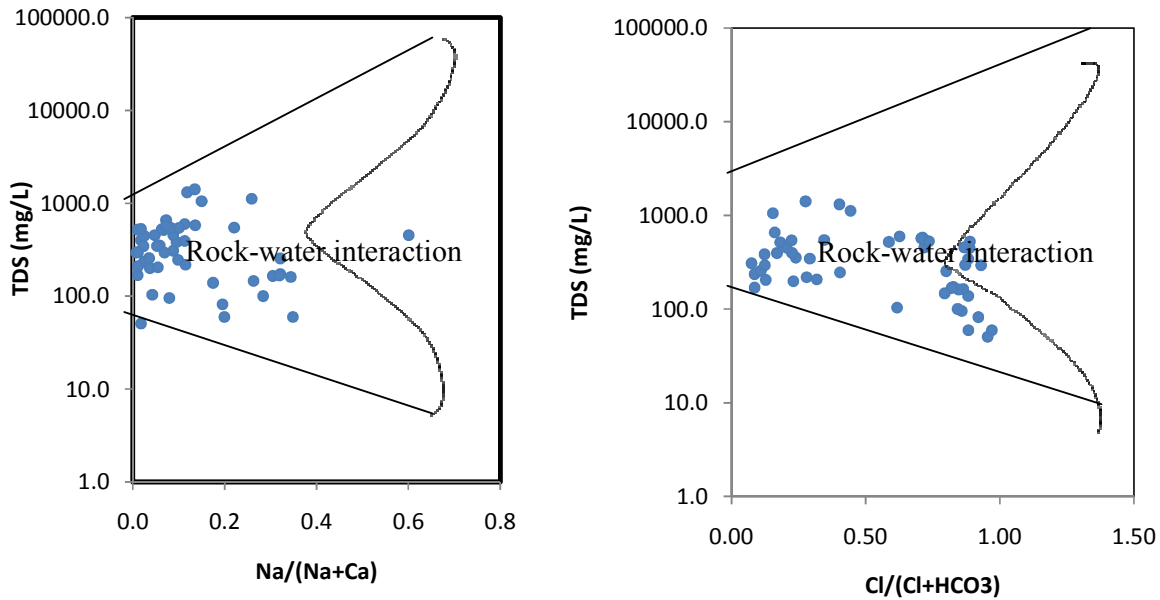
Fig. 4: Relation Na/(Na + Ca) vs TDS and between Cl/(Cl+HCO$_3$) vs TDS diagrams indicating water-rock interaction

Origin of major ions
Dominant reactions and the geochemical process that controls the groundwater chemistry were assessed by employing the scatter diagrams, ionic signatures and mechanisms controlling the water chemistry diagrams (e.g Figs. 4, 5, and 6) . The potential for a chemical reaction to occur within an aquifer was determined by calculating the chemical equilibrium of the water with the mineral phases in question. The results show that nearly all the samples were undersaturated with respect to gypsum and christobalite, and oversaturated with respect to dolomite and calcite (Fig. 5). It implies that the waters are likely to precipitate calcite and dolomite, while they are undersaturated with respect to gypsum and christobalite.

(a)

(b)

(c)

(d)
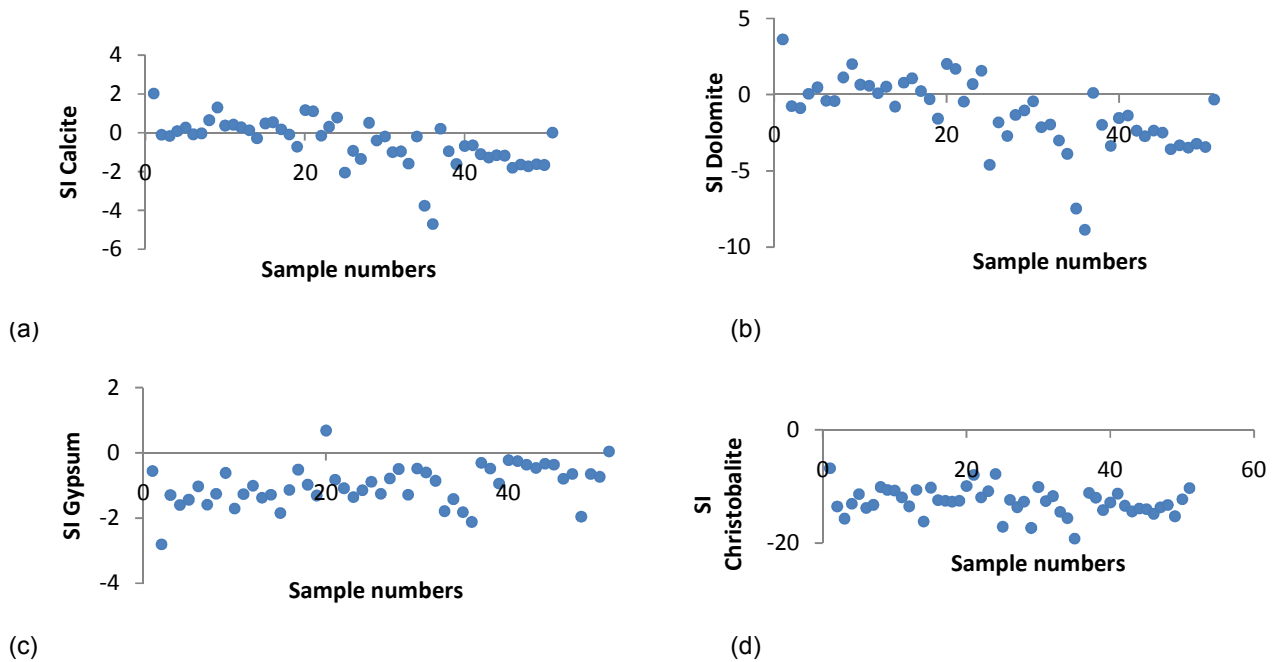
Fig. 6: Saturation indices for carbonate and silicate minerals

Sodium and Potassium

Sodium was the dominant cation found in the groundwater of the study area. Generally the dissolution of halite in water releases equal concentrations of sodium and chloride into solution such that the Na/Cl molar ratio is approximately equal to one, whereas a ratio greater than one is typically interpreted as Na released from other processes such as silicate weathering reaction. The Na^+ vs Cl^- scatter diagram (Fig. 6) shows most of the samples above the 1:1 equiline, suggesting no halite dissolution (Lakshmanan et al., 2003). The molar ratio of Na/Cl for groundwater samples of the study area generally ranges from 0.11 – 9.09 (Fig. 6). Samples having Na/Cl ratio greater than one indicate excess sodium, which might have come

from silicate weathering which is dominant in the aquifer materials of the study area. If silicate weathering is a probable source of sodium, the groundwater samples would have HCO_3^- as the most dominant abundant anion (Rogers, 1989). This is because the reaction of feldspar minerals with carbonic acid in the presence of water releases HCO_3^- (Elango et al., 2003). Table 1 shows that HCO_3^- is the dominant anion in the groundwater of the study area, hence silicate weathering was the primary process responsible for the release of Na^+ into the groundwater. However, samples with a Na/Cl ratio around and less than one indicate the possibility of some other chemical processes, such as ion exchange (Elango et al., 2003).
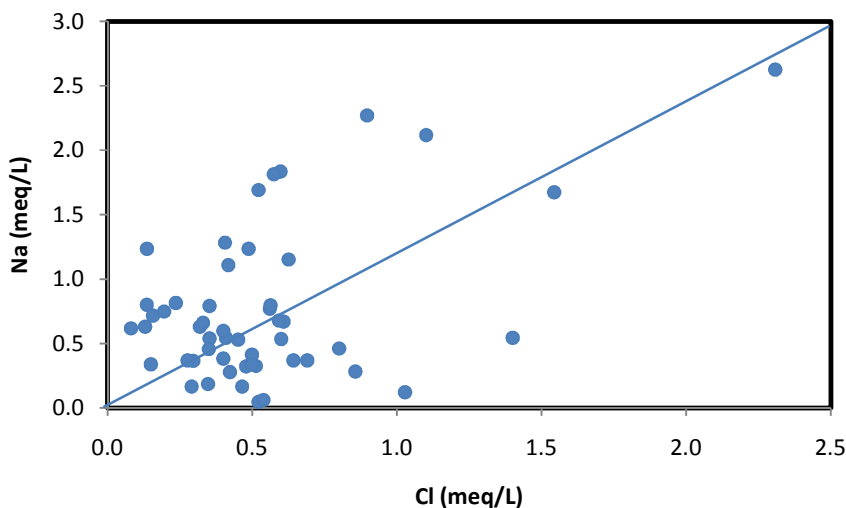

Fig. 6: Relation between Na^+ versus Cl^- in the groundwater in the study area

To further know the major functional source of dissolved solids in the groundwater, the chemical data of the groundwater samples of the study area was illustrated in Ca^{2+} + Mg^{2+} vs HCO_3 diagram (Fig. 7). Figure 7 shows that most data points fall above the 1:1 equiline, indicating predominance of alkali earth by silicate weathering over bicarbonate, which further confirms the role of silicate weathering as the primary mechanism for the occurrence of dissolved salts in the groundwater. Minor representations are noted in the bicarbonate zone due to the reaction of the feldspar

minerals with carbonic acid in the presence of water, which releases HCO_3 (Elango et al., 2003). Furthermore, the cation contribution to the groundwater by silicate weathering was also estimated using the (Na+K)/total cations index (Stallard and Edmond, 1983). The (Na+K) vs total cations (TC) scatter diagram (Fig. 8) shows sample points falling both along and above the equiline. This suggests that the cations in the groundwater might have been derived from silicate weathering (Lakshmanan et al., 2003).
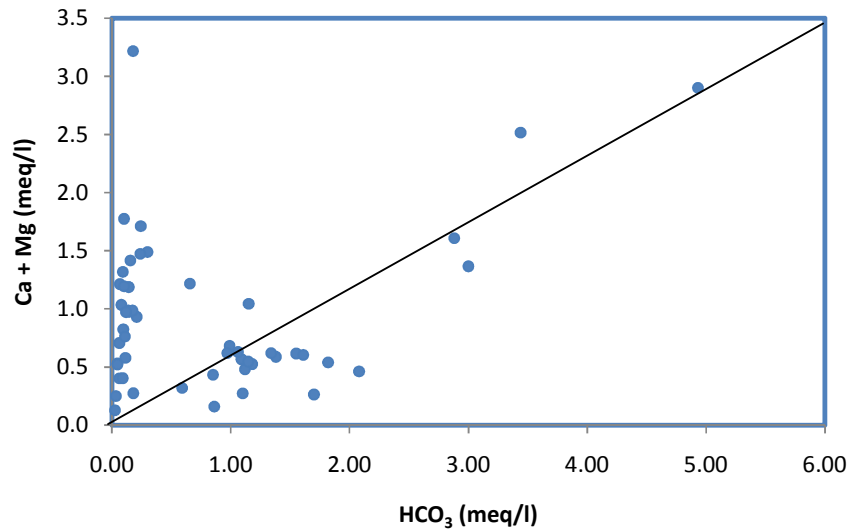
Fig. 7: Ca + Mg versus HCO$_3$ scatter diagram indicating silicate weathering

Datta and Tyagi (1996) observed that the contribution of cations may be derived from silicate weathering when (Na + K) = 0.5TC. In this case, however, the concentration of (Na + K) is about 52% of the total cations. To further evaluate and interpret the possibility that the processes of silicate weathering and/or cation exchange significantly affects groundwater composition from recharge zone to discharge zone, a bivariate plot of Ca^{2+} + Mg^{2+} - HCO$_3$ – SO$_4$ as a function of Na$^+$ + K$^+$ - Cl$^-$ were examined (Fig. 9). In the absence of these reactions, all data should plot close to the origin (McLean et al., 2000). If these processes are significant composition controlling processes, the relation between these two parameters should be linear with a slope of -1.

Figure 9 indicates an increase in Na$^+$ + K$^+$ related to a decrease in Ca^{2+} + Mg^{2+} or an increase in HCO$_3$ + SO$_4$. All data plot close to a straight line with a slope of -0.776, indicating that some of the Na$^+$, Ca^{2+} and Mg^{2+} participate in the ion exchange reaction (Garcia et al., 2001). Thus, ion exchange is also responsible for the increase of Na$^+$ from recharge zone to discharge zone. The contribution of potassium to the groundwater in these samples is modest (Table 1). Potassium might have come from the weathering of feldspar and clay minerals from the aquifer matrix as feldspars are more susceptible to weathering and alteration than quartz in silicate rocks. One possibility is illite that occurs in the soils of the region (Amadi et al., 1987).
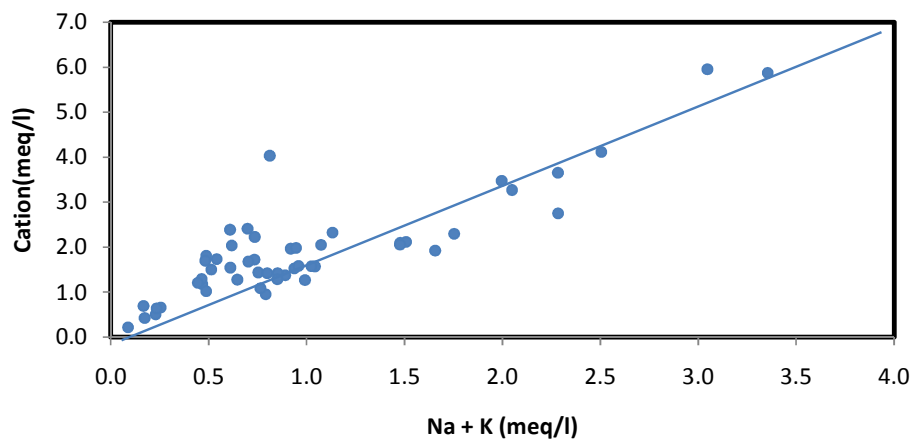

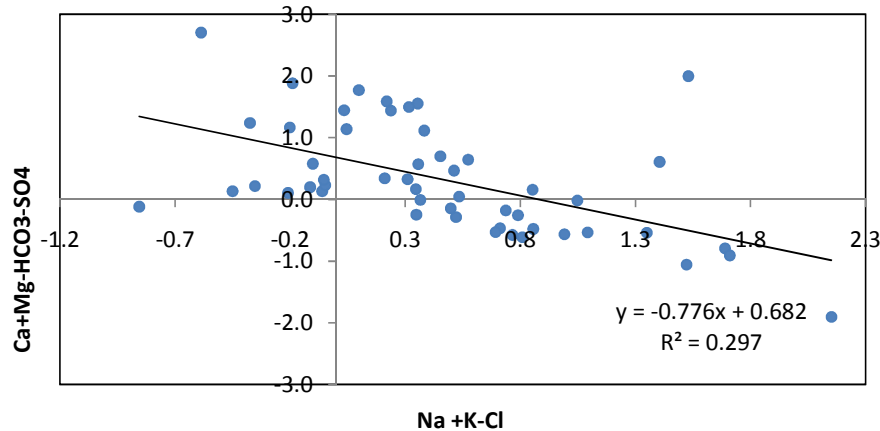**Fig. 8:** Na + K vs TC (total cations) scatter diagram indicating silicate weathering

Fig. 9: Ca-Mg-HCO$_3$-SO$_4$ versus Na + K – Cl values in the groundwater samples of the study area

Calcium and Magnesium
Calcium ion was the dominant cation next to sodium in the groundwater of the study area. Calcium concentration is less than 45mg/L in all samples. Figure 7 shows the scatter diagram of Ca^{2+} + Mg^{2+} vs HCO$_3^-$. It is observed that majority of the samples lie above the 1:1 line indicating predominance of alkali earth by silicate weathering over bicarbonate (Srinivasamoorthy et al., 2008). Excess calcium and magnesium is most likely derived from the weathering of silicate minerals such as plagioclase, pyroxene, amphibolites and montmorrillonite common in the study area (Amadi et al. 1987). Cerling et al. (1989); Fisher and Mulican, 1997 observed that the plot of Ca^{2+} + Mg^{2+} vs SO$_4$ + HCO$_3^-$ is a major indicator to identify ion exchange process. If ion exchange is the process, the points tend to shift to the right side of the plot due to an excess of SO$_4$ + HCO$_3^-$. If

reverse ions exchange is the process, points tend to shift to the left side due to excess of Ca + Mg over SO$_4$ + HCO$_3^-$. The plot of the Ca^{2+} + Mg^{2+} vs SO$_4$ + HCO$_3^-$ (Fig. 10) in the study area shows that most of the groundwater samples of the alluvial aquifer are clustered around and above the 1:1 line, indicating reverse-ion exchange (El-Sayed et al., 2012).

Bicarbonate, Chloride and sulphate
The HCO$_3^-$ is derived mainly from the soil zone CO$_2$ at the time of weathering of minerals of the parent rocks. The soil zone in the subsurface environment contains elevated CO$_2$ pressure due to the decay of organic matter and root respiration, which in turn, combines with rain water (H$_2$O) to form HCO$_3^-$ (Subba Rao and Surya Rao 2010).
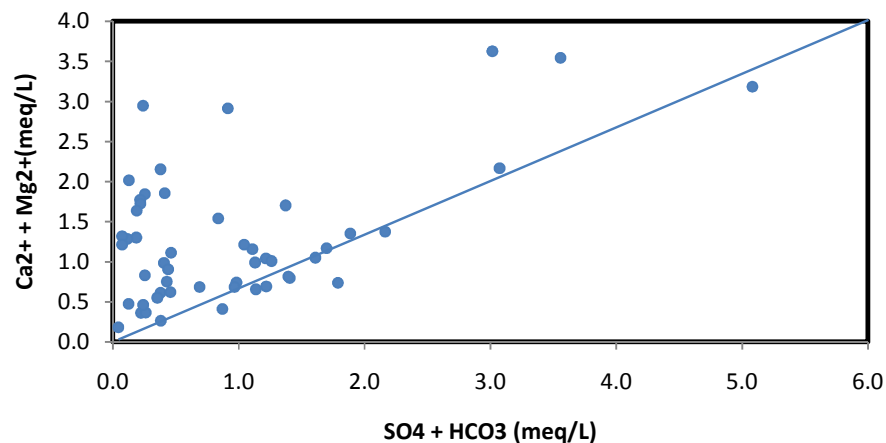

Fig.10. Ca + Mg vs HCO$_3$ + SO$_4$ values in the groundwater samples of the study area

The HCO$_3^-$ can also be derived from the dissolution of silicate minerals by H$_2$CO$_3$. The reaction of

feldspar minerals with carbonic acid in the presence of water is another possible of source of HCO$_3^-$ (Elango et

al., 2003). Chloride was the second dominant anion present in the groundwater of the study area. Its concentration ranges from 2.9 – 54.8mg/L. The origin of chloride was from the leaching of the upper soil layers, and domestic wastes (Lakshmanan et al., 2003). Sulfate concentration in the groundwater is generally less than 30mg/L. The area is characterised by shallow water table, underlain by organic rich (often peaty) wetland sediments which enhances the growth of pyrite. The SO_4^{2-} load in the groundwater might have been derived from the oxidation of sulphides associated with the peaty wetland deposits (Elango and Rannan, 2007). Additionally, sulphate might have been derived from the breakdown of organic substances of weathered soils.

Ion exchange

This process depends on replacement of adsorbed ions by ions in solution. According to Schoeller, (1967), the ion exchange between the groundwater and host environment during residence or travel can be understood by studying the chloro- alkaline indices CAI - 1 and CAI -2. Chloro- alkaline indices CAI -1 and CAI -2 was calculated using Eq. 1 and 2.

$$CAI-1=[Cl^--(Na^++K^+)]/Cl^- \qquad (1)$$
$$CAI-2=[Cl^--(Na^++K^+)]/(SO_4+HCO_3+CO_3+NO_3) \qquad (2)$$

All values are expressed in meq/L. When there is base exchange between Na^+ or K^+ with Mg^{2+} or Ca^{2+} in the groundwater, CAI -1 and CAI -2 are both positive and if a reverse ion exchange prevailed then both indices will be negative (Schoeller, 1967). Schoeller indices values of the groundwater samples of the study area (Table 1) shows that about 75% of the groundwater samples have negative values and thus exhibit a reverse ion exchange suggesting that reverse ion exchange is a prominent reaction that controls the hydrogeochemistry of the study area.

CONCLUSION

Generally, the groundwater of the study area is dominated by sodium and bicarbonate ions. Ca-Cl, Ca-HCO_3 and Na-HCO_3 are the dominant facies present in the area. The Schoeller index values are negative in about 75% of samples showing cation-ion exchange. Over 70% of the groundwater samples fall in C2 –S1 and C3 – S1 fields of the US salinity diagram and thus found to be suitable for irrigation purposes. Interpretation of the hydrogeochemical data suggests that the chemical composition of groundwater within the study area is strongly influenced by rock water interaction, dissolution and deposition of silicate minerals which is supported by high Na/Cl ratio and Gibbs diagrams, and reverse ion exchange processes. Weathering of silicate minerals control major ions such as sodium, calcium, magnesium and potassium in groundwater in the study area. The calculated SI of minerals indicates oversaturation and undersaturation of silicate and carbonate minerals.

ACKNOWLEDGEMENTS

REFERENCES

Akpokodje, E. G., 1986. A method of reducing the cement content of two stabilized Niger Delta soils. Quarterly Journal of Engineering Geology, London, (19): 359-363.

Amadi, P. A., Ofoegbu, C. O and Morrison, T., 1987. Hydrogeochemical assessment of groundwater quality in parts of the Niger Delta, Nigeria. Environmental Geology and Water Science (14): 195-202.

Amajor, L. C., 1991. Aquifers in the Benin Formation (Miocene – Recent), Eastern Niger Delta, Nigeria. Lithostratigraphy, Hydraulics and water quality. Environmental Geology & Water Science 17 (2): 85 – 101.

Andre, L., Franceschi, M., Pouchan, P and Atteia, O., 2005. Using geochemical data and modelling to enhance the understanding of groundwater flow in a regional deep aquifer, Aquitaine Basin, south west of France. Journal of Hydrology 305: 40 – 62.

APHA., 1995. Standard methods for the examination of water and waste water (17th ed). Washington, D. C.: American Public Health Association.

Cerling, T. E., Pederson, B. L and Damm, K. L. V., 1989. Sodium – Calcium ion exchange in the weathering of shales: implications for global weathering budgets. Geology (17): 552 – 554.

Chow, V. T., 1964. Handbook of Applied Hydrology, New York: McGraw-Hill.

Datta, P. S and Tyagi, A. K., 1996. Major ion chemistry of groundwater in Delhi area: Chemical weathering processes and groundwater flow regime: Journal of Geological Society of India (47): 179-188.

Davis, S. N and De Wiest, R. J. M., 1966. Hydrogeology, New York: Wiley.

Dufor, C. N and Becker, E., 1964. Public water supplies of the 100 largest cities in the US. Geological Survey water supply paper 1812: 364.

Durotoye, B., 1989. Quaternary sediments in Nigeria: In C.A. Kogbe (Ed.), Geology of Nigeria, Rock View (Nigeria) Ltd. Publishers, Jos,

Elango, L., Rannan, R and Senthil, K. M., 2003. Major ion chemistry and identification of hydrogeochemical processes of groundwater in a part of Kancheepuram district, Tamil Nadu, India. Journal of Environmental Geosciences (10): 157 – 166.

Elango, L and Rannan, R., 2007. Rock-water interaction and its control on chemical composition of groundwater. In D. Sarkar, Datta, R. &

Hannigan, R. (eds), Developments in Environmental Science (5): 229-243.

El-Sayed, M. H., Moustafa, M., El-Fadl, M. A and Shawky, H., 2012. Impact of hydrochemical processes on groundwater quality, Wadi Feiran, South Sinai, Egypt. Australian Journal of Basic and Applied Sciences (6): 638-654.

Fisher, R. S., Mulican, W. F., 1997. Hydrochemical evolution of sodium-sulfate and sodium-chloride groundwater beneath the Northern Chihuahuan desert, Trans Pecos, Rexas, USA. Hydrogeology Journal (10): 455 – 474.

Garcia, M. G., del v Hildalgo, M and Blessa, M. A., 2001. Geochemistry of groundwater in the alluvial plain of Tucuman province, Argentina. Hydrogeology Journal (9): 597 – 610.

Gibbs, R. J., 1970. Mechanisms controlling World,s water chemistry.Science 170: 1088-090.

Karanth, K. R., 1989. Hydrogeology. McGraw-Hill, New Delhi.

Kumar, M., Kumari, K., Singh, U. K and Ramanathan, A., 2009. Hydrogeochemical processes in the groundwater environment of Muktsar, Punjab: conventional graphical and multivariate statistical approach. Environmental Geology, 57, 873 – 884.

Lakshmanan, E., Kannan, K and Senthil Kumar, M., 2003. Major ion chemistry and identification of hydrogeochemical process of groundwater in part of Kancheepuram district, Tamilnadu, India. Journal of Environmental Geosciences 10 (4): 157 – 166.

McLean, W., Jankowski, J and Levitt, N., 2000. Groundwater quality and sustainability in an alluvial aquifer, Australia. In O. Sililo et al., (Eds), Groundwater, past achievements and future challenges, Rotterdam: Balkema, pp. 567 – 573.

Ofoegbu, C. O., 1985. A review of the geology of the Benue Trough, Nigeria. Journal of African Earth Science (2): 283 – 291.

Okiongbo, K. S and Douglas, R. K., 2013. Hydrogeochemical analysis and evaluation of groundwater quality in Yenagoa City and environs, Southern Nigeria. Ife Journal of Science (15): 209 - 222.

Parkhaurst, D. L and Appelo, C. A. J., 1999. User's guide to PHREEQC (version 2) – a computer programme for speciation, batch reaction, one-dimensional transport, and inverse geochemical calculations. US Geological survey water resources investigations report, 99-4259.

Rogers, R. J., 1989. Geochemical comparison of groundwater in areas of New England, New York, and Pennsylvania. Groundwater (27): 690-712.

Schoeller, H., 1967. Qualitative evaluation of groundwater resources. In Methods and techniques of groundwater investigation and development. Water Research, Series-33: UNESCO, pp. 45 – 52.

Short, K. C and Stauble, A. J., 1967. Outline of the geology of the Niger Delta. Bull. AAPG. (51): 761- 779.

Srinivasamoorthy, K., Chidambaram, S., Prasanna, M. V., Vasanthavihar, M., Peter, J and Anandhan, P., 2008. Identification of major sources controlling groundwater chemistry from hard rock terrain – A case study from Mettur taluk, Salem district, Tamil Nadu, India. Journal of Earth System science (117): 49 – 58.

Stallard, R. F and Edmond, J. M., 1983. Geochemistry of the Amazon , the influence of geology and weathering environment on the dissolved load. Journal of Geophysical Research (88): 9671 – 9688.

Subba Rao, N and Surya Rao, P., 2010. Major ion chemistry of groundwater in a river basin:

World Health Organisation (WHO)., 2004. Guidelines for drinking water quality: incorporating 1st and 2nd vol. 1 recommendations 3rd ed., Geneva.